

Raman Spectroscopy Investigation on Semi-curve Woven Fabric-graphene Synthesized by the Chemical Vapor Deposition Process

Krishna Bahadur Rai and Ram Phul Yadav

Department of Physics, Patan Multiple Campus, Tribhuvan University, Kathmandu, Nepal.

Doi: <https://doi.org/10.47011/15.2.7>

Received on: 31/10/2020;

Accepted on: 04/02/2021

Abstract: Graphene is a single layer of two-dimensional carbon atoms bound in a hexagonal lattice structure with zero band gap semiconductor. Chemical vapor deposition (CVD) is one of the most promising, inexpensive and readily ways for synthesizing monolayer pristine graphene. We have synthesized monolayer graphene shaped in semi-curve woven fabric-graphene (SWF-G) on SiO₂/Si substrate. Using Raman spectroscopy, we studied the central suspended portion (i.e., 1-6) of it exerting compression (stress) to the graphene supported on the substrate. The concentration of hole impurities on either side of the central position of semi-curve woven fabric-graphene (SWF-G) is more than on its central position. The variation of such hole doping concentration results in an upshift of 2D peak position (pos(2D)) which is opposite for high electron doping even if there is no intentional control of doping. The synthesized graphene is a single-layer high-quality new structure graphene.

Keywords: Semi-curve woven fabric-graphene, Raman spectroscopy, Charge impurities, Compression, Doping.

Introduction

Graphene is a two-dimensional single layer of carbon atoms bound in a hexagonal lattice structure with zero band gap semiconductor [1]. Graphene is now further expected to play an important role in future nanoscience and nanotechnology due to its exceptional electrical conductivity, high carrier mobility, high thermal conductivity, high optical transparency and super-hydrophobicity [2]. Chemical vapor deposition (CVD) is one of the most promising, inexpensive and readily ways for fabricating high-quality and large-area graphene. The synthesis of monolayer pristine graphene using CVD method across thin copper (Cu) foil of any size presents interesting possibilities for structural techniques. Graphene is formed based on the principle of decomposition of methane gas over a Cu substrate typically held at 1020 °C and of low solubility of carbon in Cu, such that the growth is self-limited to a single layer of

graphene [3]. There are different structures of graphene, like long twisted graphene tube in millimeter length with self-supportive, partially collapsed and vertically suspended graphene [4], graphene microtubings [5], 3-D pillared graphene [6] and plane graphene, that have different chemical, electrical and mechanical properties.

The ionized impurities such as Na⁺ on the silica (SiO₂) film and charged impurities introduced during the transfer process of CVD graphene induce charge puddles [7]. The impurities existing in the graphene-covered SiO₂/Si wafer strongly influence the electronic properties of graphene [8, 9, 10]. The silanol (SiOH), a hydrophilic film formed on a SiO₂/Si wafer, easily attracts polar adsorbates such as water molecules and causes carrier doping in the graphene after being transferred onto SiO₂/Si

wafer [11, 12, 9]. The chemical functionalization is used to shift the Fermi energy of graphene through charge transfer [7] as well as to introduce the energy band gap in a designed manner. This chemical functionalization rate and yield can be altered by using different supporting substrates [13]. An experiment suggests that when graphene is transferred onto the hydrophobic film such as polydimethylsiloxane (PDMS), the number of impurities and defects created by chemical molecules can be reduced [14]. Charge transfer complexes can be used for room-temperature deintercalation of metal atoms located between graphene and a substrate, so that the electronic properties of graphene are controlled [15]. However, research findings on the existence of doping with charge impurities and charge puddles in the semi-curve woven fabric-graphene (SWF-G or sometimes written as SGWF-G) on SiO₂/Si substrate have not been found. Along with this, it was a big challenge to tailor and assemble graphene into well-defined configuration such as SWF-G due to the lack of scalable assembly method for graphene nanostructure. In this research, we have studied the doping due to charge impurities on the different positions of SWF-G along with its way of new structure.

Experimental Details

CVD is the most useful technique for the synthesis of high-quality and large-area monolayer graphene. In this work, we used a thin foil of Cu with a thickness of 25 micrometers (μm) and a copper wire woven mesh (CWWM) having a diameter of 56 μm (Alfa-Aesar). Then, the CWWM made up using

56- μm diameter was kept over the 25- μm thickness Cu foil, as shown in schematic Fig. 1(a). Fig. 1(b) represents the schematic figure of semi-circular copper wire for the synthesis of CVD graphene. The template shown in Fig. 1(a) was employed into the thermal CVD silica chamber for the subsequent growth of SWF-G. In the initial phase, the chamber pressure was maintained at about 10^{-2} Torr and then Argon (Ar) gas was let into it at the rate of 99 sccm (sccm – standard cubic centimeters per minute) together with heating till the temperature reached 950 °C. The chamber was again adjusted to reach the temperature of 1020 °C and then Hydrogen (H₂) gas was started to pass through it at the temperature of 1003 °C for 1 hour at the rate of 99 sccm. After 1 hour cleaning with the H₂ gas at 1020 °C temperature, methane (CH₄) gas was passed into the hot-silica chamber with a gas flow rate of 21 sccm for 15 minutes at around 9.7 Torr pressure such that the system carried out the growth of SWF-G on the copper wire woven mesh-copper template. Finally, the sample was cooled rapidly at room temperature under Ar ambient atmosphere. The SWF-G/copper wire woven mesh-copper was spin-coated with polymethylmethacrylate (PMMA) followed by copper etching with ferric chloride (FeCl₃). Then, this PMMA/SWF-G was rinsed with deionized (DI) water more than five times (for approximately 30 minutes each). PMMA on the top of SWF-G was removed with the help of acetone for about 30 minutes used after the PMMA/SWF-G was transferred onto a bare SiO₂/Si wafer. At last, the sample of SWF-G/SiO₂/Si was cleaned by rinsing it into the DI water for more than five times again.

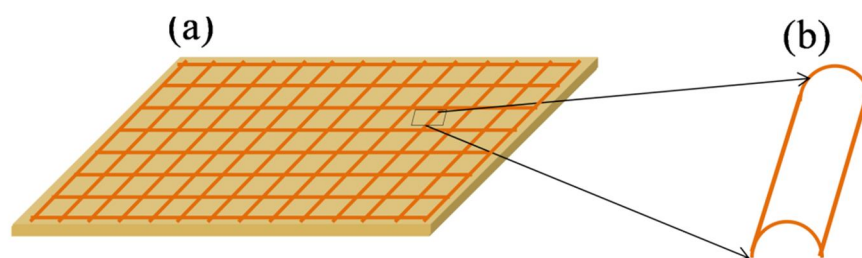


FIG. 1. (a) Schematic figure of copper foil with a thickness of 25 μm and copper wire woven mesh with a diameter of 56 μm placed over a copper foil. (b) Schematic figure of semi-circular copper wire for the synthesis of CVD graphene.

Results and Discussion

Raman spectroscopy is a sensitive tool for distinguishing single layer, bilayer and multi-layer graphene and for detecting the electronic

properties of graphene [16]. It is also sensitive to defects [17], carrier doping level [18] and strains [19]. Here, we used Raman system (InViva) with 1800 lines/mm grating, 532 nm excitation laser with 50X objective lens to confirm graphene

layer and charge impurities. The laser power was kept sufficiently lower than the damage threshold of graphene to avoid any heat-induced effects.

Fig. 2(a) shows the optical images of SWF-G/SiO₂/Si and it contains semi-curve hollow tube-graphene. Here Fig. 2(b) clearly confirms

that the synthesized graphene shape is semi-curve hollow tube-graphene on SiO₂/Si substrate. In Fig. 2(c), the semi-curve hollow tube-graphene is assigned with the schematic semi-curve red line having different red spot positions and numbers of about 4.5 μm distance to each other for taking Raman spectrum.

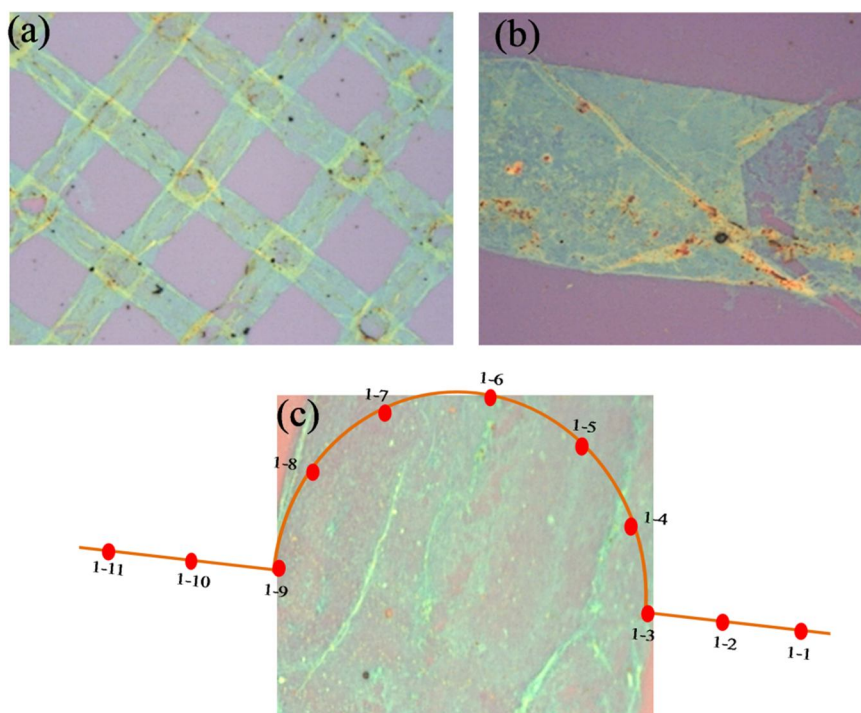
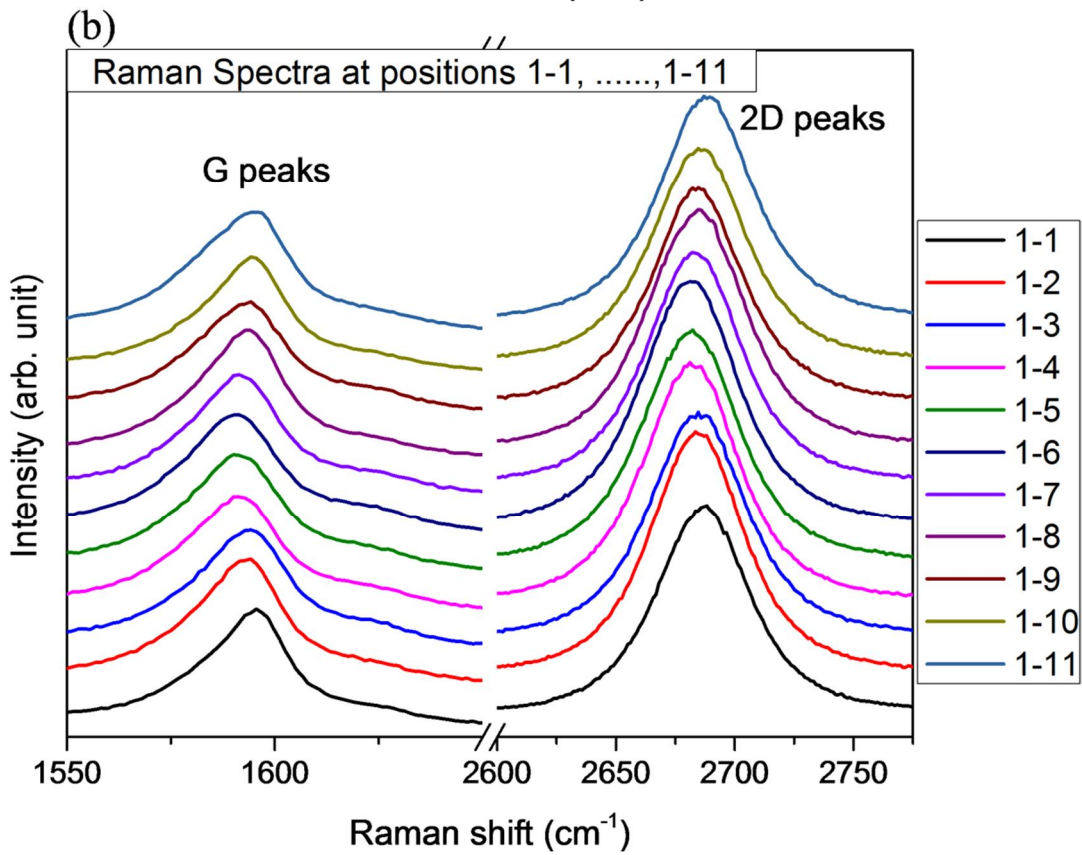
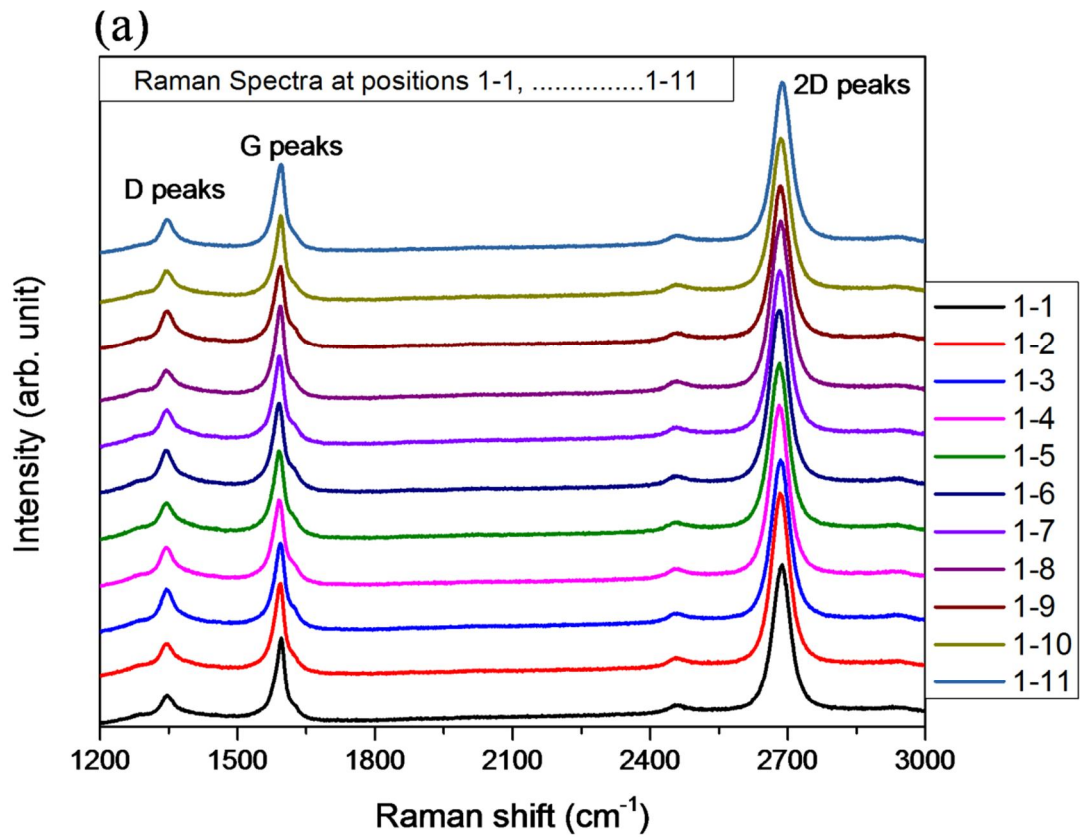


FIG. 2. (a) Woven fabric-graphene (WF-G) on SiO₂/Si. (b) Figure confirming that the synthesized graphene shape is semi-curve hollow tube graphene on SiO₂/Si substrate. (c) 11 different positions of the focused laser scanned across the semi-curve woven fabric-graphene surface on SiO₂/Si with the line mapping (red line with dot – schematic) interval of points at about 4.5 μm distance for taking Raman spectrum.

Fig. 3(a) shows the Raman spectra at 11 different positions of SWF-G with G peak position (pos(G)) and 2D peak position (pos(2D)) at $1594 \pm 4 \text{ cm}^{-1}$ and $2684 \pm 4 \text{ cm}^{-1}$, respectively, from the central position 1-6. Here, the G peak (E_{2g} mode) is related to the C-C in-plane stretching for all sp^2 carbon atoms and the 2D peak (G' mode) is related to the second-order double-resonance process [20]. Raman I_{2D}/I_G intensity ratio of the central semi-curve hollow tube graphene with the value of 1.93 to about 1.41 on either side indicates that the graphene is a monolayer graphene. In the same figure, the D peak position is $1346 \pm 3 \text{ cm}^{-1}$ on either side of position 1-6 and such D peak is the dominant sp^2 Raman signature of disorder or defects. In Fig.

3(b), pos(G) and pos(2D) peaks of 1-5, 1-4, 1-3, 1-2, 1-1 positions and 1-7, 1-8, 1-9, 1-10, 1-11 positions reveal the blue shift as compared to the pos(G) and pos(2D) peak of central position 1-6. This blue shift on either side of the central laser focused position is attributed to the compression strain [21] of semi-curve hollow tube woven fabric graphene film. The Raman spectra of pos(G) and pos(2D) peaks increase on either side of the central position in a sense that the central portion (i.e., position 1-6) of graphene is making compression stress to the graphene supported on the substrate. Slight upshifts of $\text{pos(G)} = 7 \text{ cm}^{-1}$ and $\text{pos(2D)} = 7 \text{ cm}^{-1}$ indicate a small compression.



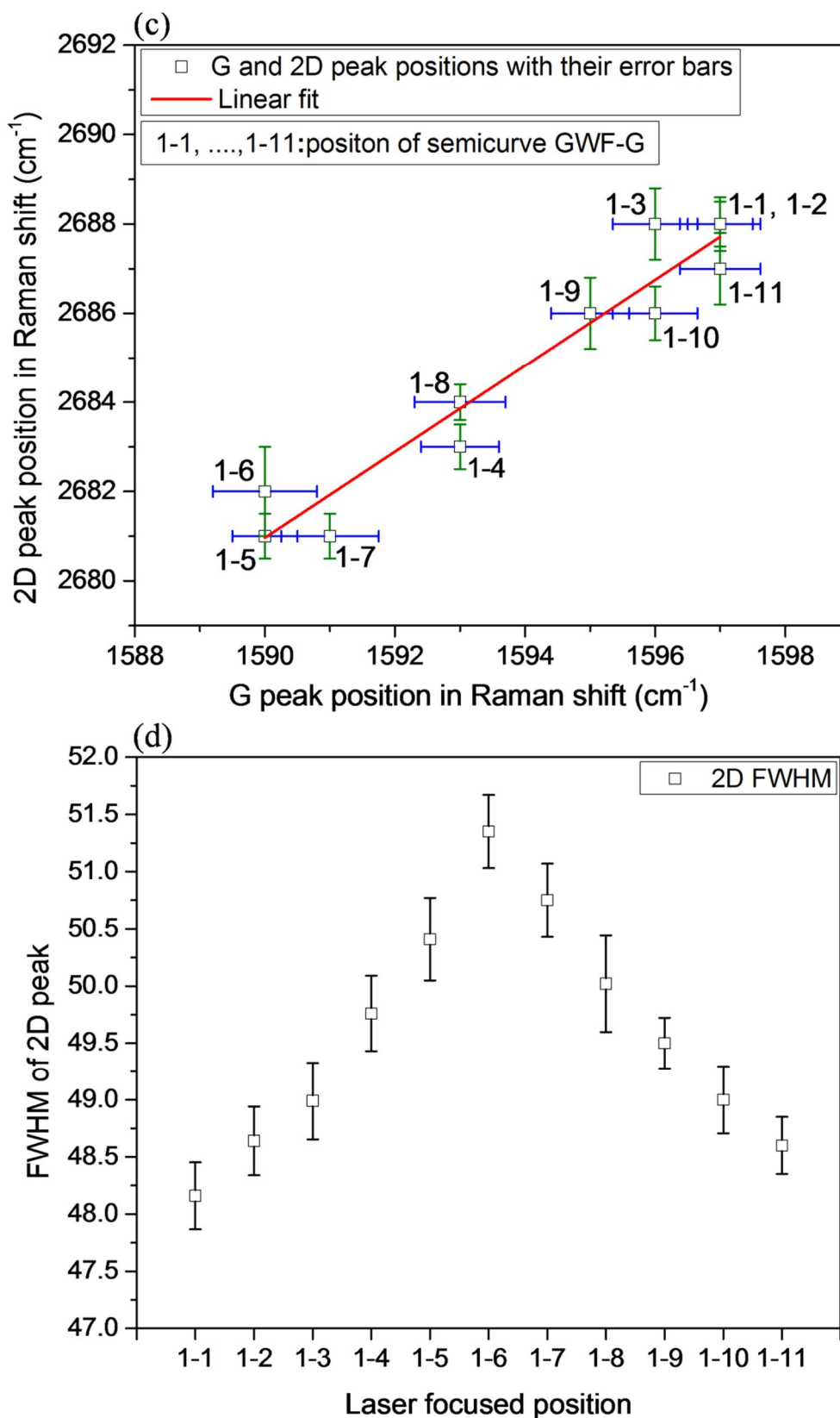
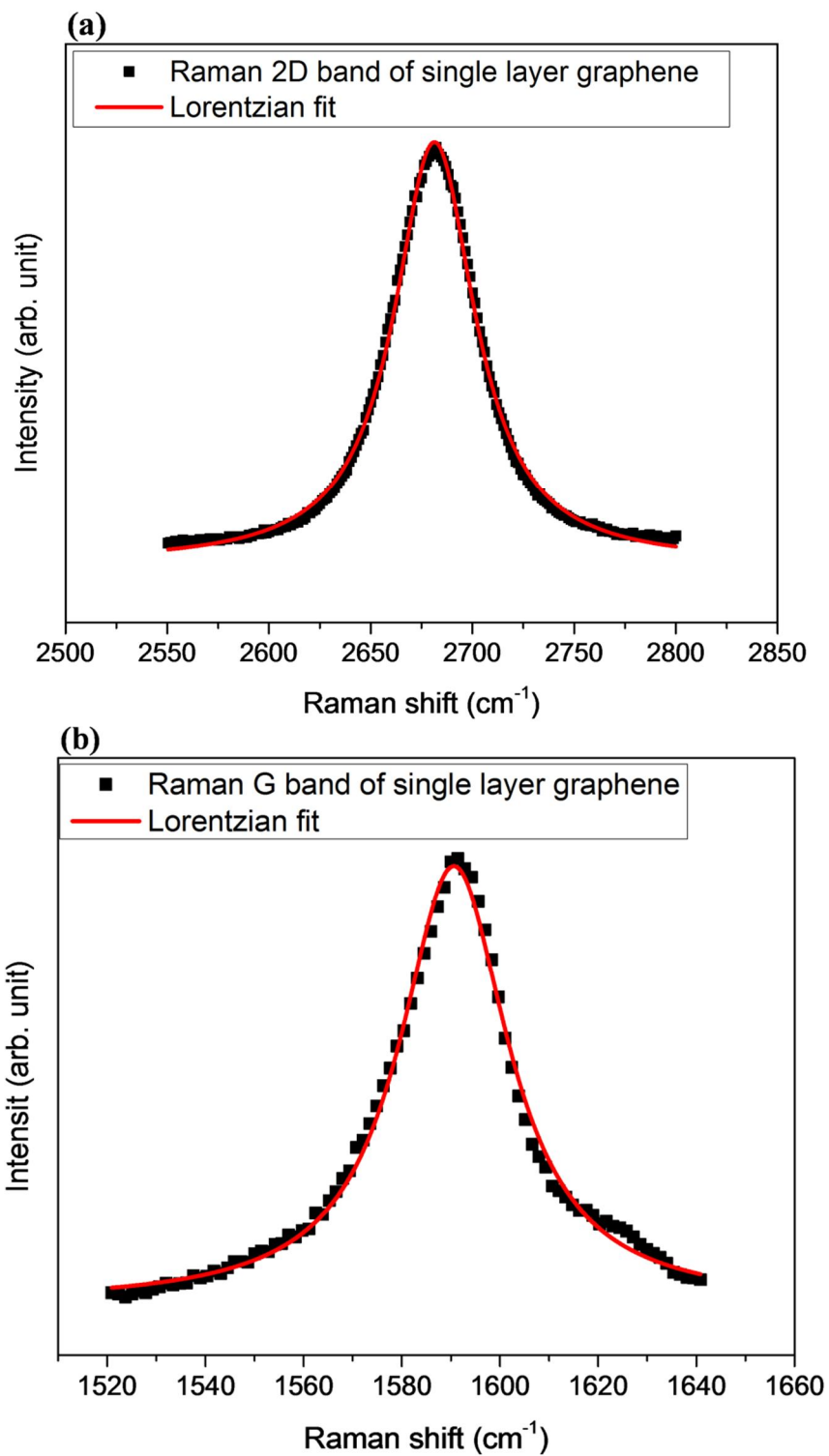


FIG. 3. (a) Raman spectra of SWF-G at 11 different positions. (b) The spectra with the G peak on the left and 2D peak on the right in which $\text{pos}(G)$ and $\text{pos}(2D)$ upshift from central position (i.e., 1-6) of SWF-G. (c) Linear fit for the $\text{pos}(G)$ and $\text{pos}(2D)$ with their blue color error bars and green color error bars for G peak position and 2D peak position, respectively. (d) FWHM of $\text{pos}(2D)$ with their error bars and laser focused at 11 different positions with a distance of about $4.5 \mu\text{m}$ to each other on the SWF-G.

The graphene sample checked here is a monolayer graphene, as it is CVD-synthesized. The integrated intensity ratio of the 2D and G peaks (I_{2D}/I_G) is related to the doping with charged impurities in which a larger I_{2D}/I_G refers to a smaller amount of charged impurities and vice versa [14]. The upshift of the G band also reflects the doping with charged impurities [22]. However, this peak shift is less sensitive to doping than the I_{2D}/I_G ratio [18]. In Fig. 3(b), the intensities of 2D peaks at different focused positions are different in which 2D peak intensities gradually decrease on either side of the central position (i.e., at 1-6), but all G peak spectra have nearly the same intensity due to the very weak substrate charged impurities effect on the G-band intensity. Fig. 3(c) has a linear fit that correlates $\text{pos}(2D)$ and $\text{pos}(G)$ with their respective error bars (blue color) for G peak position and green color error bars for 2D peak position. Like the $\text{pos}(G)$ peak, the $\text{pos}(2D)$ peak upshifts in the same excitation energy. This allows to distinguish electron - from hole - doping in graphene [23, 24]. Fig. 3(c) also shows that $\text{pos}(2D)$ peaks at different focused positions; i.e., at 1-1, 1-11, 1-2, 1-10 and 1-3, 1-9 is sensitive to doping as compared to $\text{pos}(2D)$ peaks at 1-4, 1-8, 1-5, 1-7, 1-6 positions. The variation of the $\text{pos}(2D)$ peak shift is mainly due to the hole doping resulting in an upshift and which is opposite for high-electron doping [18] even if there is no intentional control of doping. Adsorbents induced chemical doping, substrate and water could explain the p-doping [25] on positions 1-1, 1-11, 1-2, 1-10 and 1-3, 1-9. Fig. 3(d) shows the plot of 11 different laser focused positions and Full Width at Half Maximum (FWHM) of 2D peak with their error bars having values ± 0.294 for position 1-1, ± 0.301 for position 1-2, ± 0.337 for position 1-3, ± 0.33 for position 1-4, ± 0.361 for position 1-5, ± 0.319 for position 1-6, ± 0.32 for position 1-7, ± 0.422 for position 1-8, ± 0.223 for position 1-9, ± 0.294 for position 1-10 and ± 0.25 for position 1-11. From Ref. [25] and Fig. 3(c), Fig. 3(d) indicates that FWHM of 2D peak decrease corresponds to the

$\text{pos}(2D)$ peak increase on either side of position 1-6. This is quite similar to what we observed in intentionally doped graphene, where the Fermi energy was modulated using a gate [26].

In Fig. 4(a), the Raman 2D band was fitted with Lorentzian-shaped curve at various positions of the SWF-G sample. The symmetric shape and narrow width of the 2D band [27] suggest that the synthesized graphene is in fact of a single layer and the situation background of graphene quality is understood. Since the Raman spectrum of graphene is on the SiO_2 substrate and there is no fluorescence effect, this 2D band Lorentzian has the phonon flat background. Raman spectrum in Fig. 4(b) shows Lorentzian line shape fit of the G peak of single-layer graphene. Fig. 4(c) has FWHM of G peak and Ref. [28] studied that the peak $\text{pos}(G)$ band in Fig. 3(c) and FWHM of G band have an inverse relation in monolayer-graphene sample. Fig. 4(d) shows the G peak position and the I_{2D}/I_G ratio as a function of position of laser focused points in SWF-G (or SGWF-G). The different I_{2D}/I_G ratios at different positions are: at position 1-1, $I_{2D}/I_G = 1.41$, at position 1-2, $I_{2D}/I_G = 1.42$, at position 1-3, $I_{2D}/I_G = 1.64$, at position 1-4, $I_{2D}/I_G = 1.78$; at position 1-5, $I_{2D}/I_G = 1.9$, at position 1-6, $I_{2D}/I_G = 1.93$, at position 1-7, $I_{2D}/I_G = 1.89$, at position 1-8, $I_{2D}/I_G = 1.79$, at position 1-9, $I_{2D}/I_G = 1.6$, at position 1-10, $I_{2D}/I_G = 1.41$ and at position 1-11, $I_{2D}/I_G = 1.4$. This clearly shows a large variation with hole doping: at low doping, the 2D peak intensity is stronger than the G peak intensity such that I_{2D}/I_G ratio is 1.93 (maximum) at that central position 1-6 and this is due to the no-substrate effect on the top of semi-curve hollow graphene. The decreases in maximum I_{2D}/I_G ratio on either side corresponds to the blue shift in the 2D peaks [29] for other laser focused positions. At high doping, the I_{2D}/I_G ratio is low and corresponds to 1.41 at position 1-1, while at position 1-11, $I_{2D}/I_G = 1.4$. This may indicate that the doping on the graphene is due to the charge transfer from the underlying substrate SiO_2/Si .



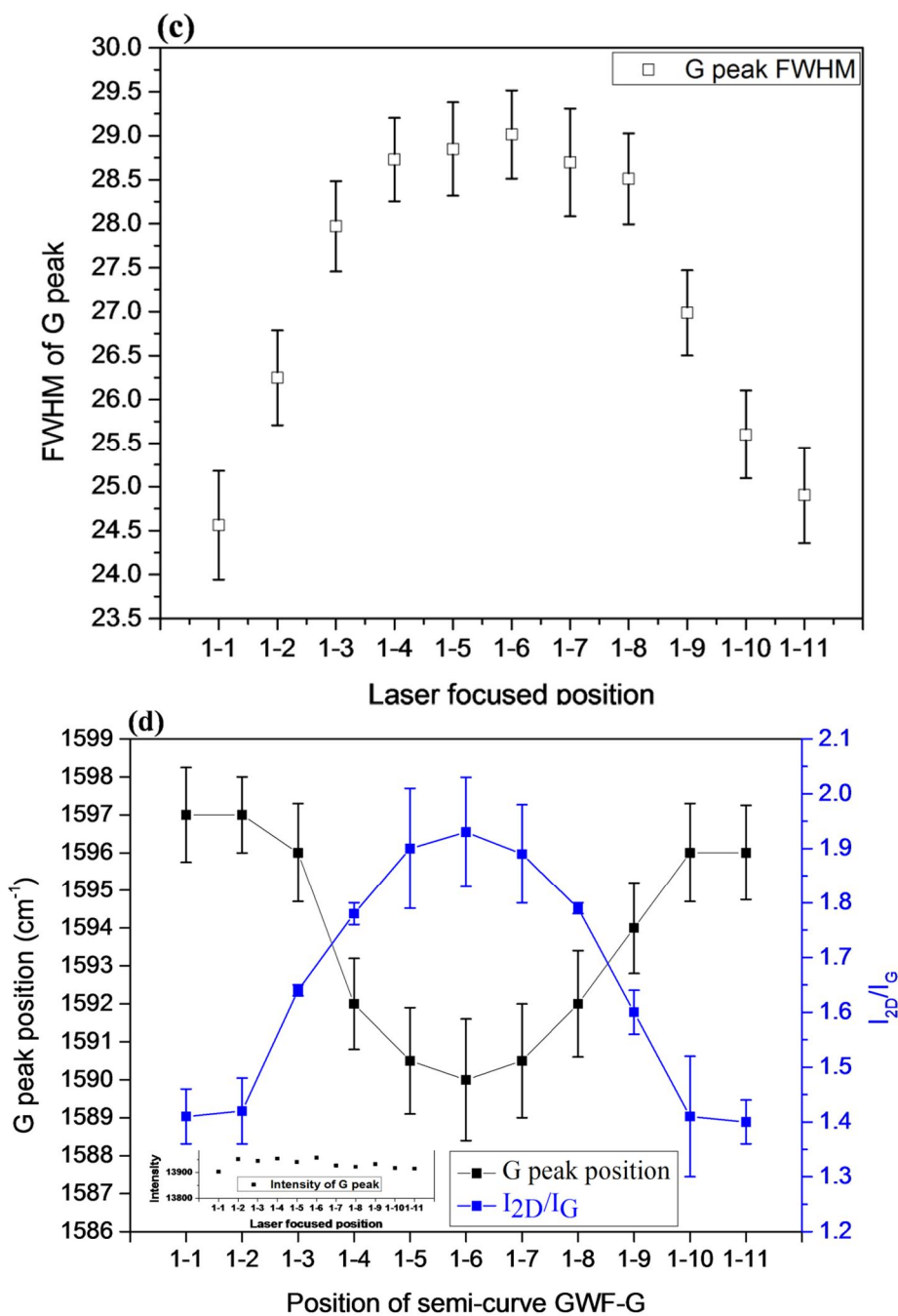


FIG. 4. (a) Raman spectrum (black dot line) of SWF-G fitted by Lorentzian fitting (red line). (b) Lorentzian fit of the G peak. (c) FWHM and its error bars for G peak at 11 different positions. (d) Pos(G) and I_{2D}/I_G ratio as function of 11 different laser focused positions of SWF-G or SGWF-G. An inset in the bottom left of the figure contains nearly the same intensity of the G peak.

Conclusions

We presented a systematic analysis of the Raman spectra of deposited semi-curve woven fabric-graphene on SiO_2/Si substrate. The increasing pos(G) and pos(2D) peak on either side of the central portion (i.e., position 1-6) of graphene is making compression (stress) to the graphene supported on the substrate. The large variation in Raman parameters is assigned to

inhomogeneous unintentional hole doping from substrate's charge impurities. In particular, we show how graphene doping levels vary within the same flake depending on the distance between the graphene and substrate. Such structure of graphene (SWF-G) might have future applications on supercapacitor and hydrogen energy storage devices.

References

- [1] Novoselov, K.S., Geim, A.K., Morozov, S.V., Jiang, D., Zhang, Y., Dubonos, S.V., Grigorieva, I.V. and Firsov, A.A., *Science*, 306 (2004) 666.
- [2] Zhu, Y., Murali, A., Cai, W., Li, X., Suk, J.W., Potts, J.R. and Ruoff, R.S., *Adv. Mater.*, 22 (2010) 3906.
- [3] Polat, E.O., Balci, O., Kakenov, N., Uzlu, H.B., Kocabas, C. and Dahiya, R., *Sci. Rep.*, 5 (2015) 16744.
- [4] Rai, K.B., *Int. J. Adv. Eng.*, 2(2) (2019) 31.
- [5] Hu, C., Zhao, Y., Cheng, H., Wang, Y., Dong, Z., Jiang, C., Zhai, X., Jiang, L. and Qu, L., *Nano Lett.*, 12(11) (2012) 5879.
- [6] Gosh, K., Yue, C.Y., Moniruzzaman, S.K. and Jena, R.K., *Appl. Mater. and Interfaces*, 9(18) (2017) 15350.
- [7] Fan, X., Nouchi, R., Tanigaki, K., *J. Phys. Chem. C*, 115 (2011) 12960.
- [8] Jimenez-Villacorta, F., Climent-Pascual, E., Ramirez-Jimenez, R., Sanchez-Marcos, J., Prieto, C. and Andres, A.D., *Carbon*, 101 (2016) 305.
- [9] Lafkioti, M., Krauss, B., Lohmann, T., Zscheschang, U., Klauk, H., Klitzing, K.V. and Hosono, H., *Nano Lett.*, 10 (2010) 1149.
- [10] Kreil, D., Haslhofer, M. and Bohm, H.M., *Lithuanian Journal of Physics*, 59(1) (2019) 35.
- [11] Lee, D.E., Ahn, G. and Ryu, S., *J. Am. Chem. Soc.*, 136 (18) (2014) 6634.
- [12] Brandenburg, J.G., Zen, A., Fitzner, M., Ramberger, B., Kresse, G., Tsatsoulis, T., Gruneis, A., Michaelides, A. and Alfe, D., *J. Phys. Chem. Lett.*, 10 (2019) 358.
- [13] Wang, Q.H., Jin, Z., Kim, K.K., Hilmer, A.J., Paulus, G.L. C., Shih, C.J., Ham, M.H., Sanchez-Yamagishi, J.D., Watanabe, K., Taniguchi, T., Kong, J., Jarrilo-Herero, P. and Strano, M.S., *Nat. Chem.*, 4 (2012) 724.
- [14] Rai, K.B., Khadka, I.B., Kim, E.H., Ahn, S.J., Kim, H.W. and Ahn, J.R., *J. Korean Phys. Soc.*, 72 (1) (2018) 107.
- [15] Shin, H.C., Ahn, S.J., Kim, H.W., Moon, Y., Rai, K.B., Woo, S.H. and Ahn, J.R., *Appl. Phys. Lett.*, 109 (2016) 081603.
- [16] Bayle, M., Reckinger, N., Huntzinger, J.R., Felten, A., Bakaraki, A., Landois, P., Colomer, J.F., Henrard, L., Zahab, A.A., Sauvajol, J.L. and Paillet, M., *Phys. Status Solidi B*, 252 (11) (2015) 2375.
- [17] Ferrari, A.C. and Basko, D.M., *Nat. Nanotechnol.*, 8 (2013) 235.
- [18] Kim, S.J., Park, S.J., Kim, H.Y., Jang, G.S., Park, D.J., Park, J.Y., Lee, S. and Ahn, Y.H., *Appl. Phys. Lett.*, 108 (2016) 203111.
- [19] Mueller, N.S., Heeg, S., Alvarez, P.M., Kusch, P., Wasserroth, S., Clark, N., Schedin, F., Parthenios, J., Papagelis, K., Galiotis, C., Kalbac, M., Vijayaraghavan, A., Huebner, U., Gorbachev, R., Frank, O. and Reich, S., *2D Mater.*, 5 (2017) 015016.
- [20] Jorio, A., Dresselhaus, M.S., Saito, R. and Dresselhaus, G., "Raman Spectroscopy in Graphene-related System", 1st Edn., (Weinheim Wiley, 2011).
- [21] Ding, J., Fisher, F.T. and Yang, F.H., *J. Vac. Sci. Technol. B*, 34 (2016) 051205.
- [22] Ni, Z.H., Yu, T., Luo, Z.Q., Wang, Y.Y., Liu, L., Wong, C.P., Miao, J., Huang, W. and Shen, Z.X., *ACS Nano*, 3 (3) (2009) 569.
- [23] Bruna, M., Ota, A.K., Ljas, M.I., Yoon, D., Sassi, Y. and Ferrai, A.C., *ACS Nano*, 8 (7) (2014) 7432.
- [24] Mazeikiena, R., Niaura, G., Eicher-Lorka, O. and Malinauskas, A., *Chemija*, 30 (2) (2019) 78.
- [25] Schedin, F., Geim, A.K., Morozov, S.V., Hill, E.H., Blake, P., Katsnelson, M.I. and Novoselov, K.S., *Nat. Mater.*, 6 (2007) 652.
- [26] Pisana, S., Lazzeri, M., Casiraghi, C., Novoselov, K.S., Geim, A.K., Ferrai, A.C. and Mauri, F., *Nat. Mater.*, 6 (2007) 198.
- [27] Woehrl, N., Ochedowski, O., Gottlieb, S., Shibasaki, K. and Schulz, S., *AIP Adv.*, 4 (2014) 047128.
- [28] Casiraghi, C., Pisana, S., Novoselov, K.S., Geim, A.K. and Ferrai, A.C., *Appl. Phys. Lett.*, 91 (2007) 233108.
- [29] Oh, T., *Trans. on Electrical and Electronic Mater.*, 14 (5) (2013) 246.